

**ASSESSING FUNCTIONAL VASODILATION
IN THE GRACILIS COLLATERAL ARTERIOLE**

A Senior Project

Presented to

The Faculty of the Biomedical Engineering Department

California Polytechnic State University,

San Luis Obispo

In Partial Fulfillment

Of the Requirements for the Degree

Bachelor of Science in Biomedical Engineering

by

Megan T. Chu

August 2015

PROJECT INFORMATION

TITLE: Assessing Functional Vasodilation in the
Gracilis Collateral Arteriole

AUTHOR: Megan T. Chu

DATE SUBMITTED: August 2015

ADVISOR: Dr. Trevor Cardinal, Associate Professor

ABSTRACT

Assessing Functional Vasodilation in the Gracilis Collateral Arteriole

Megan Chu

Peripheral arterial occlusive disease (PAOD) involves arterial occlusion due to the formation of atherosclerotic plaques. It is suggested that intermittent claudication, the most frequent clinical presentation of PAOD, is caused by impaired vasodilation. Current treatments for PAOD are not directed at improving vascular reactivity and are often insufficient. Stimulating arteriogenesis in collateral arterioles has therapeutic potential for PAOD, but because arterioles are the primary site of blood flow resistance, it is important that these treatments do not impair collateral vasodilation. Before this can be evaluated, the effects of arteriogenesis on collateral function must be studied in untreated collaterals. There is impaired functional vasodilation at the collateral stem following collateral enlargement in the mouse hindlimb ischemia model. In order to determine if a similar impairment occurs at the collateral midzone, visualization of the gracilis collateral arteriole must be improved. In this study, we tested the hypotheses that FITC-dextran injected into the intravascular space would allow visualization of the gracilis collateral arteriole using epifluorescence, and that a trans-illumination device placed deep to the gracilis muscle would allow visualization of the arteriole by backlighting the midzone. Both of these methods allowed for clear visualization of the gracilis vasculature. Additionally, the placement of the trans-illumination device did not affect vasodilation in the upstream feed artery, suggesting that collateral reactivity would also remain unaltered by the device. In future studies, both of these visualization techniques will be employed to assess functional vasodilation in the midzone of the gracilis collateral arteriole in both unoperated animals and those with ligation-induced ischemia.

ACKNOWLEDGEMENTS

I would like to thank Dr. Cardinal for his guidance throughout the duration of this project, and for always letting me tag along on his walks between classes to bombard him with questions.

Then, many thanks to the rest of the MaVR lab for their help and support, and for always letting me vent and pretending to laugh at my nerdy science humor. You guys are awesome.

I would also like to express my gratitude to the Hannah-Forbes Fund for funding this project in particular and, more generally, for making so many student projects possible.

Finally, I would like to thank my parents for showing me their continued love and patience while also pushing me to achieve my potential, even when I don't want to hear it.

“If we knew what it was we were doing, it would not be called research, would it?”

- Albert Einstein

TABLE OF CONTENTS

LIST OF FIGURES	vi
INTRODUCTION	1
Peripheral Arterial Occlusive Disease	1
Arteriogenesis	2
Vasculature Visualization Techniques	4
Objective	6
METHODS	7
Animal Preparation	7
Functional Vasodilation	7
Effects of Trans-Illumination Device Insertion on Functional Vasodilation	8
Collateral Visualization with Trans-illumination	9
Collateral Visualization with FITC-Dextran	9
Data Analysis	9
RESULTS	10
DISCUSSION	13
REFERENCES.....	17
APPENDICES.....	20

LIST OF FIGURES

Figure 1. Peripheral Arterial Occlusive Disease (PAOD)	1
Figure 2. Gracilis Collateral Circuit	4
Figure 3. Trans-illumination Device Placement	8
Figure 4. Trans-illumination Device Insertion Does Not Affect Vasodilation	10
Figure 5. Gracilis Collateral Arteriole with Trans-illumination	11
Figure 6. Gracilis Collateral Arteriole after FITC-Dextran Injection	12

INTRODUCTION

Peripheral Arterial Occlusive Disease

Peripheral arterial occlusive disease (PAOD) affects eight to ten million Americans, causing 500,000 hospitalizations and 100,000 angiograms in the United States annually [1]. This condition is associated with increased risk of myocardial infarction, stroke, and vascular death. PAOD is most commonly caused by atherosclerotic plaques that build up in the arteries and restrict blood flow to the downstream tissue (**Figure 1**).

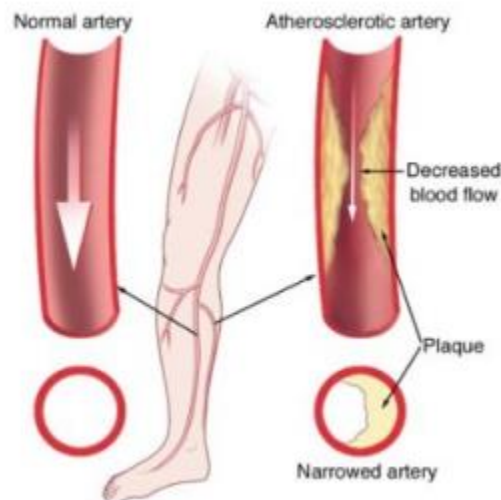


Figure 1. Peripheral arterial occlusive disease (PAOD). PAOD is characterized by atherosclerotic plaques that form inside arteries and decrease blood flow to the tissue [2].

Ankle-brachial index (ABI), which is the ratio of the highest systolic blood pressure in the lower limb to that of the arm, is commonly used for the diagnosis of PAOD ($ABI < 0.9$) [3]. The most severe form of PAOD is critical limb ischemia (CLI, $ABI < 0.4$), which is present in 12 percent of the adult population and is characterized by ischemic pain at rest [1]. CLI occurs due to inadequate blood flow to the lower limbs and thrombotic complications, and often results in limb loss [3]. Before the disease progresses to this point, the most frequent clinical presentation of PAOD is intermittent claudication ($ABI = 0.4-0.9$), or leg pain that occurs with exertion but not at

rest [4]. One proposed cause for intermittent claudication is impaired vascular reactivity. When L-arginine was used to restore NO synthesis, and consequently, endothelium-dependent vasodilation, claudication symptoms in PAOD patients improved [5]. Additionally, supervised exercise conditioning in patients with PAOD led to an increase in treadmill exercise performance as well as reduced claudication pain during exercise [6]. That exercise training improves claudication symptoms indicates impaired vasodilation as a cause of intermittent claudication.

Current treatments for PAOD include pharmacological therapy, endovascular intervention by angioplasty or stenting, and bypass grafting. Anti-platelet and anti-inflammatory medications such as pentoxifylline are considered minimally effective, producing only small improvements in walking distance of patients, while vasodilators such as cilostazol improve walking distance but cannot be used in patients with heart failure [6]. Peripheral bypass therapy improves treadmill exercise performance and functional status in patients with claudication [6]. However, bypass therapy for claudication has high short-term costs in terms of morbidity, mortality, and health care [6]. Many patients who undergo bypass grafting end up with bypass occlusion and CLI, resulting in a greater risk of limb loss and the need for additional procedures. The goal of both surgical and pharmacological therapies is to counteract the negative effects of atherosclerosis. However, none of these treatments aim to improve vascular reactivity.

Arteriogenesis

Although they do lead to improvement in some patients, the current approaches to treating PAOD are often insufficient, and developing therapies based on processes that occur naturally in the body are promising. Pre-existing collateral networks can function as natural bypasses around an occlusion to restore blood flow. A blockage in an artery leads to a decrease in pressure downstream of the occlusion, which increases the pressure gradient across the collateral. This

increase in shear stress causes these arterioles to increase in diameter through the process of arteriogenesis [7]. Following endothelial activation, the presentation of adhesion molecules such as ICAM is increased and monocyte chemoattractant protein-1 (MCP-1) is secreted, causing monocytes in the circulation to extravasate and differentiate into macrophages. These cells secrete a number of arteriogenic factors, including tumor necrosis factor (TNF- α) for smooth muscle cell proliferation, vascular endothelial growth factor (VEGF) for endothelial cell proliferation, and matrix metalloproteinases (MMPs) for basement membrane and matrix degradation. Smooth muscle cells and fibroblasts are responsible for the synthesis of a new matrix [8].

Arteriogenesis is important because of its therapeutic potential for the treatment of PAOD, but the development of therapies to stimulate arteriogenesis warrants investigation into the impact of these treatments on collateral vasodilation, as the collateral circulation is the primary site of blood flow resistance in the ischemic limb and proper control of blood flow is necessary to meet the metabolic demands of the tissue. However, this can only occur after collateral function is studied in untreated collaterals during and after arteriogenesis.. Chronic ischemia causes impaired functional vasodilation in the collateral stem due to collateral enlargement through mechanoadaptation [9,10]. It is important to investigate the effects of arteriogenesis on vasodilation in the collateral midzone to determine if similar impairment is observed.

A common animal model for PAOD is the mouse hindlimb model, where a collateral network is present in the gracilis muscle (**Figure 2**).

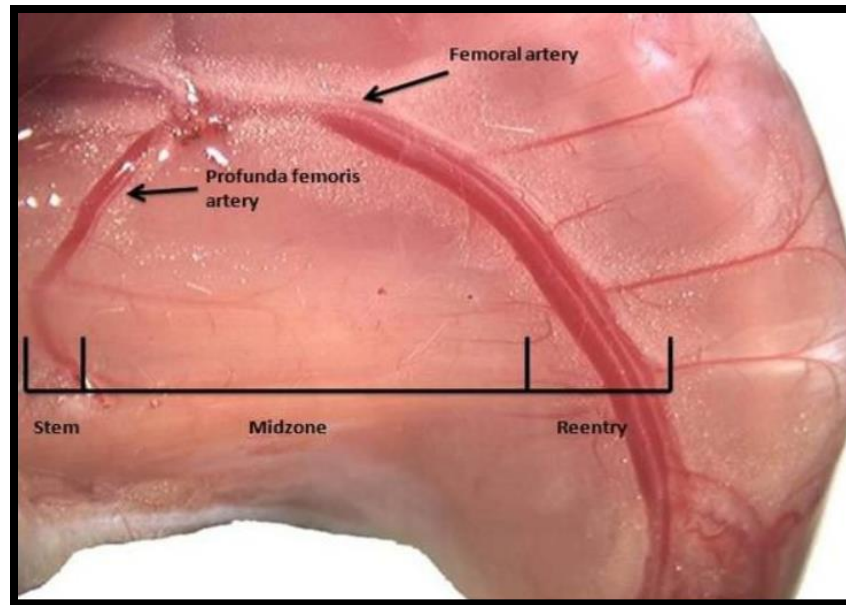


Figure 2. Gracilis Collateral Circuit. The three sections of the gracilis collateral circuit in the mouse hindlimb.

However, the gracilis tissue is relatively thick as well as optically dense, and the collateral arteriole is located deep within the muscle. This leads to poor visualization of the arteriole, making it difficult to gauge the vasodilation of the vessel in response to a stimulus.

Vasculature Visualization Techniques

There are different techniques that are currently employed to visualize blood vessels in vivo. First, laser speckle imaging can be used to create detailed vasculature maps based on optical scattering during blood flow [11]. A low-power laser generates time-integrated speckle patterns, which are converted to flow images [12]. For instance, laser speckle imaging provided high spatial resolution maps of relative blood flow in a rodent skin fold model [12]. This technique is well-suited for this model because the large vessel diameters (50-200 μm) allow for flow monitoring over a wide field of view [12]. Laser speckle imaging is particularly useful in tissues with superficial vessels [12], but optical scattering diminishes the ability to visualize subsurface microvasculature [13], which could be the case for the arteriole in the gracilis muscle.

Another technique that allows for the visualization of vasculature in vivo is sidestream dark field (SDF) imaging. The probe used in this imaging modality consists of a central light guide surrounded by light emitting diodes (LEDs), which illuminate the microcirculation by scattering [14]. The emission wavelength of the LEDs is 530 nm, so that the scattered green light is absorbed by hemoglobin in the red blood cells of superficial vessels at a tissue depth of up to 3 mm [15]. The physiological cross-sectional area of the gracilis anterior is $1.1 \pm 0.5 \text{ cm}^2$ [16]. Assuming a circular cross-sectional area, the muscle radius is about 3.3 mm and the muscle diameter is about 6.7 mm. Therefore, SDF imaging may not allow for deep enough penetration to effectively visualize the gracilis collateral arteriole. Additionally, microcirculatory alterations may be induced by the pressure from the application of the probe onto the tissue surface [14].

Other attempts to visualize blood vessels in vivo utilize fluorescein isothiocyanate-conjugated dextran (FITC-dextran), which is a fluorescent dye that emits green light when excited. To assess vascular permeability in mice, varying molecular weights of FITC-dextran were injected into the bloodstream [17]. At low molecular weights, fluorescence intensity decreased in the blood vessel area and increased in the interstitial space; however, at high molecular weights, the dextran remained in circulation [17]. Based on this disparity, high-molecular weight FITC-dextran was delivered by retro-orbital injection to improve visualization of retinal blood vessels, and successfully allowed for the quantification of neovascularization area [18]. Injection of FITC-dextran at a high molecular weight may also improve visualization of the gracilis collateral arteriole enough to measure vasodilation.

Another technique for blood vessel visualization involves the use of trans-illumination. In a study exploring a novel method for in vivo trans-illumination, the mouse cremaster muscle was surgically isolated from the surrounding tissue in vivo so that it could be placed on a transparent

pedestal of silastic rubber during continuous superfusion of a physiological salt solution and trans-illuminated with an intravital microscope [19,20]. While this preparation made use of the trans-illumination capabilities of a microscope outside the body of the anesthetized animal, it is also possible to create a device specifically for trans-illumination in microcirculatory regions that are more difficult to access. In an in vivo flow cytometry study, the mouse ear was trans-illuminated with a device containing a green LED to identify the proper blood vessel location for the flow cytometry measurements [21]. In the mouse ear, the blood vessels are about 70-100 μm from the surface, and the appropriate vessel size range for trans-illumination is roughly 20-50 μm [21]. Because the gracilis collateral arteriole ranges from about 15-25 μm [22], trans-illumination may be a promising method for visualizing vasodilation of this arteriole in response to a stimulus.

Objectives

The goal of this study was to assess approaches to visualize functional vasodilation in the gracilis collateral arteriole. To achieve this goal, we tested two hypotheses:

1. FITC-dextran injected into the intravascular space will allow visualization of the gracilis collateral arteriole using epifluorescence.
2. A trans-illumination device placed deep to the gracilis muscle will backlight the midzone and allow visualization of the collateral arteriole.

Supporting either of these methods in an unoperated animal model will allow the completion of future studies to study vasodilation during and after arteriogenesis following ligation-induced ischemia.

METHODS

Animal Preparation

All experimental protocols were approved by the California Polytechnic State University Institutional Animal Care and Use Committee (IACUC). Male and female albino ICR mice were housed in a temperature-controlled environment in the University Vivarium and were provided with food, water, and enrichment (bedding, mouse house, and tunnel tube).

Mice were anesthetized in an induction chamber using 5% isoflurane in oxygen at 0.8-1.0 $l \cdot min^{-1}$. Animals were weighed and moved to a preparatory bench, where the isoflurane was decreased to 2-3% and the flow rate was adjusted as necessary. Hair was removed from the hindlimb region using depilatory cream, and skin was disinfected using chlorhexidine diacetate. Mice were then placed on a microscope stage with a heating pad that maintained body temperature at 35°C, as measured by a rectal thermistor probe.

An incision was made in the medial aspect of the hindlimb, and blunt dissection was used to expose the gracilis muscle and remove overlying fascia and connective tissue. The tissue was irrigated periodically with phosphate-buffered saline (PBS) to prevent desiccation.

Functional Vasodilation

Two tungsten microelectrodes were placed near the motor-end plate of the gracilis muscle, halfway between the profunda and the saphenous arteries. A data acquisition unit (ADInstruments PowerLab) and digital chart recording software (LabChart) were used to stimulate muscle contraction with 1 mA square waves with a duration of 200 μs and a frequency of 1 Hz, to optimize electrode placement for maximal localized gracilis contraction. The exposed

area was then irrigated with PBS and covered with plastic wrap, and the preparation equilibrated for 30 minutes.

After the equilibration period, images of the profunda femoris artery were captured using an intravital microscope (Olympus BXFM) and digital imaging software (QCapture Pro). Then, the muscle was stimulated for 90 seconds with 1 mA square waves with a duration of 200 μ s and a frequency of 8 Hz. Starting immediately after stimulation, images of the profunda were captured every minute until it returned to its resting diameter.

Effects of Trans-Illumination Device Insertion on Functional Vasodilation

Using blunt dissection, a pocket was created deep to the anterior and posterior gracilis muscles. After electrode placement and equilibration, described above, functional vasodilation was assessed at the profunda femoris. Then, the electrodes were removed and the polydimethylsiloxane-coated LED trans-illumination device was placed in the pocket deep to the gracilis muscles (**Figure 3A-B**), followed by a second electrode placement, equilibration period, and vasodilation measurement.

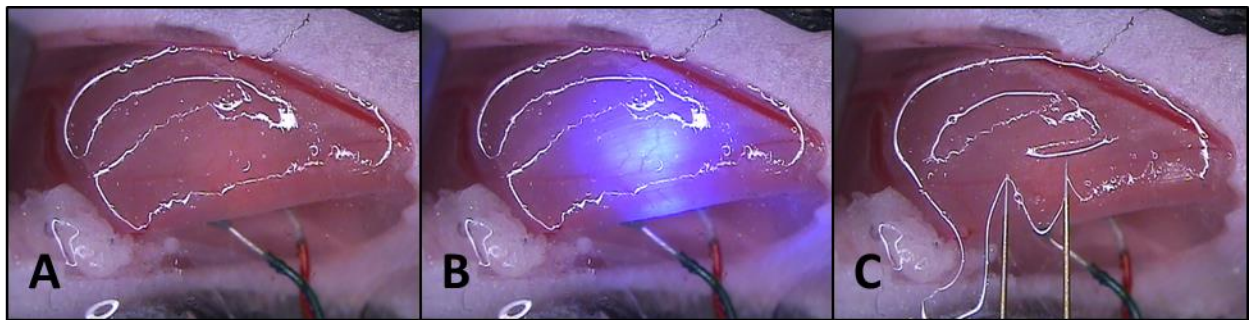


Figure 3. Trans-Illumination Device Placement. The LED trans-illumination device was inserted under the anterior and posterior gracilis muscles (A). When turned on, the light was used to backlight the muscle for better visualization of the collateral arteriole in the gracilis anterior (B). Electrodes were placed on the gracilis muscle in the location shown for functional vasodilation measurement (C).

Collateral Visualization with Trans-Illumination

To measure collateral vasodilation, the LED was adjusted to the desired brightness and positioned in the pocket deep to the gracilis muscles for an optimal view of the collateral arteriole midzone. After electrode placement and equilibration, described above, resting images of the midzone were captured. Then, functional vasodilation was assessed at the midzone. Images were captured every minute for ten minutes immediately following stimulation.

Collateral Visualization with FITC-Dextran

Fluorescein isothiocyanate-dextran (FITC-dextran, 250000 MW dextran, 0.1 ml) was injected intravascularly via jugular venipuncture. These experiments were performed with minimal lighting to avoid photo-bleaching the FITC-dextran. The collateral vessels in the gracilis anterior were visualized via epifluorescent illumination with an intravital microscope. Functional vasodilation was measured at the midzone of the collateral, as described above. After each experiment, mice were euthanized by cervical dislocation.

Data Analysis

ImageJ software was used to measure vessel diameter. Percent changes in diameter were calculated as the difference between the dilated and resting diameters divided by the resting diameter and multiplied by 100%. Paired t-tests were used to compare the resting and dilated diameters of the profunda femoris artery under normal conditions, after undermining the gracilis, and after inserting the trans-illumination device. ANOVA was used to detect differences in profunda diameter between the three sets of conditions, both at rest and after electrical stimulation, and also to detect differences in percent change in diameter between the three sets of conditions. Data are presented as mean \pm SE.

RESULTS

Improving the visualization of the gracilis collateral arteriole is necessary to assess functional vasodilation. In this experiment, we tested the hypotheses that either placing a trans-illumination device deep to the gracilis muscle or injecting FITC-dextran into the intravascular space would allow visualization of the collateral arteriole.

Functional vasodilation was observed in the profunda femoris artery (**Figure 4A**) following electrical stimulation of the gracilis muscle under normal conditions, after undermining the gracilis, and after inserting the LED trans-illumination device deep to the muscle (**Figure 4B-C**).

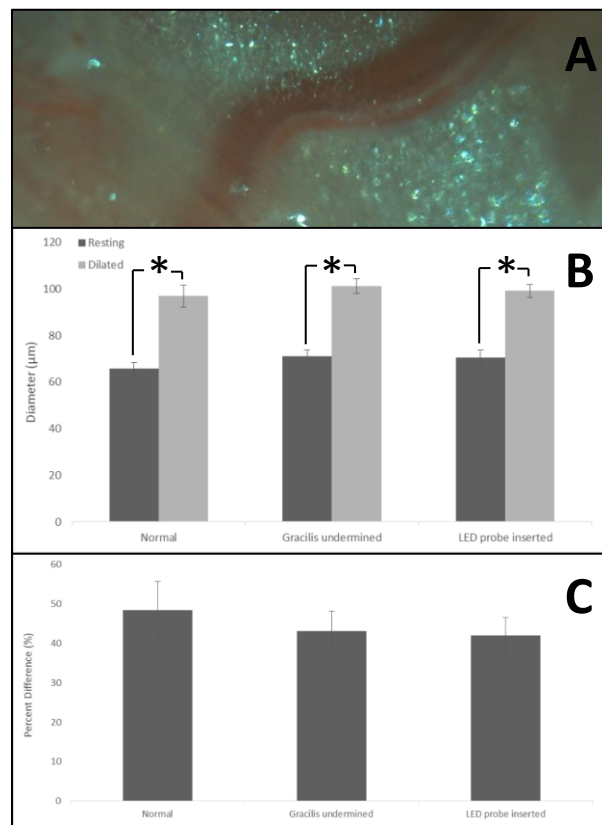


Figure 4. Trans-Illumination Device Insertion Does Not Affect Vasodilation. Vasodilation in the profunda was measured in the location shown (A) following stimulation normally, after undermining the gracilis, and after inserting the LED device. B) Vessel diameter before and after stimulation. C) Percent change in vessel diameter. Vessel diameter increased with electrical stimulation, but there was no difference in percent change between the three sets of conditions. * $p < 0.05$, $n=4$

The dilated diameter of the profunda was larger than the resting diameter in each category.

Under normal conditions, the resting diameter was $66 \pm 3 \mu\text{m}$ and the diameter after stimulation was $97 \pm 5 \mu\text{m}$. After undermining the gracilis, the diameter was $71 \pm 2 \mu\text{m}$ resting and $101 \pm 3 \mu\text{m}$ after stimulation. With the trans-illumination device inserted, the diameter was $70 \pm 3 \mu\text{m}$ resting and $99 \pm 3 \mu\text{m}$ after stimulation. Neither the resting nor the dilated diameters measured after undermining the gracilis or inserting the trans-illumination device were different from the respective values under normal conditions. The percent change in diameter with stimulation was 48 ± 7 percent under normal conditions, 42 ± 5 percent with the gracilis undermined, and 41 ± 5 percent with the trans-illumination device inserted.

Because inserting the trans-illumination device had no adverse effects on vasodilation in the profunda, it was then used to visualize the functional vasodilation of the collateral midzone. A montage of representative images of the gracilis illuminated by the LED displays the entire collateral arteriole (**Figure 5**).

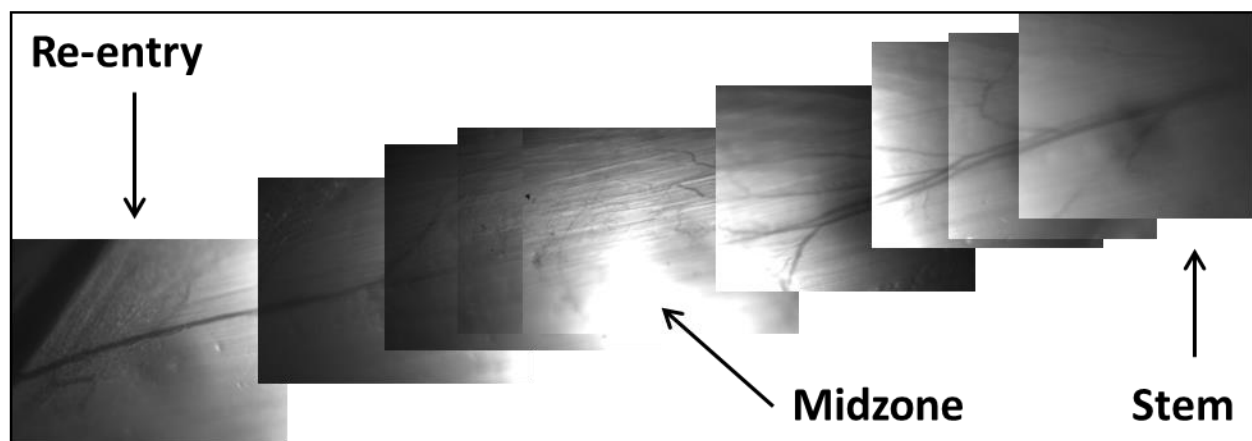


Figure 5. Gracilis Collateral Arteriole with Trans-Illumination. Images of the gracilis collateral arteriole were captured by placing a trans-illumination device deep to the muscle for improved visualization (n=3).

Trans-illuminating the gracilis muscle allowed for distinct visualization of the blood vessels. However, the LED was so bright that it obscured the view of any vasculature located directly above it, making it necessary to move the probe around to visualize different vessels. Additionally, it was difficult to distinguish the arteriole from the venule in the gracilis anterior. Although trans-illumination allowed for clear visualization, no midzone dilation was observed following stimulation in any of the replicates.

An alternative approach to enhance contrast in the gracilis muscle involved the intravascular injection of FITC-dextran to better view the collateral arteriole. After injection of the fluorescent dye, the gracilis vasculature appeared bright green (**Figure 6**).



Figure 6. Gracilis Collateral Arteriole after FITC-Dextran Injection. The stem (A), midzone (B), and re-entry (C) of the gracilis collateral circuit were imaged with fluorescence after injection of FITC-dextran (n=4).

However, despite the clarity of the gracilis muscle with epifluorescent illumination of FITC-dextran injection, it was still difficult to determine which vessel was the collateral arteriole. There was no midzone dilation observed in any of the visible vessels after electrical stimulation.

DISCUSSION

Intermittent claudication, the most frequent clinical presentation of PAOD, may be caused by impaired vasodilation. Current treatments for PAOD are not directed at improving vascular reactivity, and are often insufficient. Stimulating arteriogenesis in collateral arterioles has therapeutic potential for PAOD, but it is important that these treatments do not impair collateral vasodilation. Before this can be evaluated, the effects of arteriogenesis on collateral function must be studied in untreated collaterals. There is impaired functional vasodilation at the collateral stem following collateral enlargement in the mouse hindlimb ischemia model. To determine if a similar impairment occurs at the collateral midzone, visualization of the gracilis collateral arteriole must be improved. In this study, we tested the hypotheses that FITC-dextran injected into the intravascular space would allow visualization of the gracilis collateral arteriole using epifluorescence, and that a trans-illumination device placed deep to the gracilis muscle would allow visualization of the arteriole by backlighting the midzone.

The first method that we explored involved a trans-illuminating LED device that was placed deep to the gracilis muscles. Using this device to backlight the collateral arteriole improved contrast and allowed for visualization of the blood vessels in the area, supporting our hypothesis. However, the device required constant manipulation to clearly view different regions of the gracilis, mostly due to the brightness of the LED, which obscured any vasculature located directly above it. Future versions of the trans-illumination device could include a dimmer switch to reduce the brightness of the light. Additionally, instead of placing the device deep to the gracilis muscles, the hair could be removed from the posterior side of the hindlimb so that the device could shine through the entire limb, which would also reduce its brightness.

In order to use this technique to visualize collateral vasodilation in response to a stimulus, it was necessary to confirm that the device itself did not affect vasodilation. Neither undermining the gracilis nor inserting the trans-illumination device had an effect on functional vasodilation in the profunda. Based on this observation, it can be assumed that functional vasodilation in the collateral midzone is similarly unaffected by these methods. Future studies could be conducted to determine how large of an LED probe it would take to alter reactivity in the profunda.

In subsequent experiments performed to observe functional vasodilation in the midzone of the collateral arteriole, there was no change in diameter of the arteriole following electrical stimulation. The lack of vasodilation could be explained by visualization of the venule instead of the arteriole. However, there was also no dilation of the profunda femoris artery in the same experiments, suggesting that another factor was affecting vasodilation. Although the only reagent used was PBS, it is possible that contamination occurred. The acute inflammatory response triggered by microbial infection involves vasodilation to increase the delivery of plasma and leukocytes to the site of infection [23]. If the vessels in the gracilis collateral circuit were already dilated, they might not increase in diameter further in response to an electrical stimulus. To avoid any contamination in the future, sterile saline could be applied to the tissue in place of PBS to prevent desiccation.

After exploring trans-illumination to improve visualization, we used epifluorescence following FITC-dextran injection to visualize the gracilis collateral arteriole. FITC-dextran successfully caused the vasculature in the gracilis muscle to fluoresce, supporting our hypothesis. However, in addition to the blood vessels, the surrounding tissue also turned green, though not as brightly. This is likely due to tissue autofluorescence, which can appear green from a variety of components. For instance, lipofuscins, elastin, and collagen all have excitation spectra that

include blue and emission spectra that include green, similar to FITC-dextran [24]. Because of this, it may be beneficial to experiment with the use of a fluorescent dye other than FITC-dextran. A red dye such as tetramethylrhodamine isothiocyanate-conjugated dextran (TRITC-dextran, Sigma-Aldrich) might provide a clearer image of the hindlimb circulation with better visualization of the collateral arteriole.

Although visualization with FITC-dextran appeared promising aside from the possible autofluorescence, there were again no diameter changes in the visible gracilis vasculature after electrical stimulation. As with trans-illumination, we initially assumed that the major visible blood vessel was the venule that runs throughout the length of the gracilis. Arterioles are much more reactive than venules due to a thicker tunica media, so it was expected that vessels that changed in diameter were arterioles, while those that did not were venules. Once again, however, the profunda remained similarly unaffected by stimulation, suggesting that the lack of vasodilation was caused by another factor, potentially the contamination of a reagent such as PBS. Therefore, the visible blood vessel in the gracilis muscle could have been either the arteriole or the venule.

In future studies, it may be necessary to evaluate other indicators, instead of relying on a vasodilation response to distinguish between vessel types. For example, venule diameter is generally larger than the corresponding arteriole diameter. Then, when using a fluorescent dye such as FITC-dextran, high magnification can allow for the visualization of blood flow through the vessels. The direction of blood flow is opposite in the two vessel types, and the velocity of blood flow is generally greater in arterioles than in venules [25]. These small visual differences can be utilized in vivo to differentiate between the gracilis blood vessels.

In conclusion, visualization must be improved to measure functional vasodilation in the midzone of the gracilis collateral arteriole. Placing a trans-illumination device deep to the gracilis muscle does not affect vasodilation in the upstream feed artery, suggesting that collateral vasodilation remains unaltered as well. Trans-illumination also improves the contrast between the blood vessels in the gracilis and the surrounding tissue for clear visualization. Injecting FITC-dextran causes the blood vessels in the gracilis to fluoresce, also allowing for clear visualization of the vasculature. As a next step, either of these methods can be used to observe vasodilation in the profunda femoris artery and the gracilis collateral midzone in unoperated animals. Then, the effects of ligation-induced ischemia and arteriogenesis on vasodilation in the midzone of the collateral arteriole will be assessed using similar visualization techniques.

REFERENCES

- [1] Davies, M.G. “Critical limb ischemia: epidemiology.” *Methodist Debaque Cardiovascular Journal*. 8.4 (2012): 10-14.
- [2] Halabi, A. *The Facts About Peripheral Arterial Disease*; 2009. Available at: http://www.michiganmedicalreport.com/michigan_cardiology/details/237/podcast.aspx. Accessed August 17, 2015.
- [3] Di Minno G., G. Spadarella, G. Cafaro, et al. “Systematic reviews and meta-analyses for more profitable strategies in peripheral artery disease.” *Annals of Medicine*. 46.7 (2014): 475-489.
- [4] Swaminathan A., S. Vemulapalli, M.R. Patel, and W.S. Jones. “Lower extremity amputation in peripheral artery disease: improving patient outcomes.” *Vascular Health and Risk Management*. 10 (2014): 417-424.
- [5] Böger, Rainer H., Stefanie M. Bode-Böger, Wolfgang Thiele, Andreas Creutzig, Klaus Alexander, and Jürgen C. Frölich (1998). Restoring Vascular Nitric Oxide Formation by L-arginine Improves the Symptoms of Intermittent Claudication in Patients with Peripheral Arterial Occlusive Disease. *Journal of the American College of Cardiology* 32, 1336-344.
- [6] Nelher, Mark R., Mary M. McDermott, Diane Treat-Jacobson, Ian Chetter, and Judith G. Regensteiner. “Functional outcomes and quality of life in peripheral arterial disease: current status.” *Vascular Medicine* 8 (2003): 115-126.
- [7] Heil, M., Inka Eitenmuller, T. Schmitz-Rixen, and W. Schaper. “Arteriogenesis versus angiogenesis: similarities and differences.” *J. Cell Mol. Med*. 10.1 (2006): 45-55.
- [8] Silvestre, Jean-Sebastien, David M. Smadja, and Bernard I. Levy. “Postischemic Revascularization: From Cellular and Molecular Mechanisms to Clinical Applications.” *Physiol. Rev*. 93 (2013): 1743-1802
- [9] Cardinal, Trevor R., Kyle R. Struthers, Thomas J. Kesler, Matthew D. Yocum, David T. Kurjiaka, and James B. Hoying. Chronic Hindlimb Ischemia Impairs Functional Vasodilation and Vascular Reactivity in Mouse Feed Arteries. *Frontiers in Physiology* 2 (2011).
- [10] Struthers K. *Ischemia Impairs Vasodilation in Skeletal Muscle Resistance Artery*. San Luis Obispo: California Polytechnic State University; 2011:94. Available at: <http://digitalcommons.calpoly.edu/theses/546/>. Accessed August 7, 2015.
- [11] White, Sean M., Steven C. George, and Bernard Choi. “Automated Computation of Functional Vascular Density Using Laser Speckle Imaging in a Rodent Window Chamber Model.” *Microvascular Research* 82.1 (2011): 92–95.

- [12] Choi, Bernard, Nicole M. Kang, and J. Stuart Nelson. "Laser speckle imaging for monitoring blood flow dynamics in the in vivo rodent dorsal skin fold model." *Microvascular Research* 68 (2004): 143-146.
- [13] Choi, Bernard, Tyson L. Ringold, and Jeehyun Kim. "Methods to Enhance Laser Speckle Imaging of High-Flow and Low-Flow Vasculature." Annual International Conference of the IEEE Engineering in Medicine and Biology Society. IEEE Engineering in Medicine and Biology Society. Conference (2009): 4073–4076.
- [14] Goedhart, P.T., M. Khalilzada, R. Bezemer, J. Merza, and C. Ince. "Sidestream Dark Field (SDF) imaging: a novel stroboscopic LED ring-based imaging modality for clinical assessment of the microcirculation.," *Opt. Express* 15 (2007): 15101-15114.
- [15] Backer, Daniel De, Steven Hollenberg, Christiaan Boerma, Peter Goedhart, Gustavo Büchele, Gustavo Ospina-Tascon, Iwan Dobbe, and Can Ince. "How to Evaluate the Microcirculation: Report of a round Table Conference." *Crit Care* 11.5 (2007).
- [16] Burkholder, Thomas J., Brian Fingado, Stephanie Baron, and Richard L. Lieber. "Relationship between Muscle Fiber Types and Sizes and Muscle Architectural Properties in the Mouse Hindlimb." *J. Morphol.* 221.2 (1994): 177-90.
- [17] Egawa, Gyohei et al. "Intravital Analysis of Vascular Permeability in Mice Using Two-Photon Microscopy." *Scientific Reports* 3 (2013): 1932.
- [18] Li S., T. Li, Y. Luo et al. "Retro-orbital injection of FITC-dextran is an effective and economical method for observing mouse retinal vessels." *Molecular Vision* 17 (2011): 3566-3573.
- [19] Bagher, P., and S.S. Segal. "The Mouse Cremaster Muscle Preparation for Intravital Imaging of the Microcirculation." *J. Vis. Exp.* 52 (2011): e2874.
- [20] Georgi, M.K., J. Vigilance, A.M. Dewar, and M.D. Frame. "Terminal arteriolar network structure/function and plasma cytokine levels in db/db and ob/ob mouse skeletal muscle." *Microcirculation (New York, NY:1994)* 18.3 (2011): 238-251.
- [21] Novak, J. et al. "In Vivo Flow Cytometer for Real-Time Detection and Quantification of Circulating Cells." *Optics Letters* 29.1 (2004): 77-79.
- [22] Gallagher, R. *The Impact of Outward Remodeling on Vasodilation in Skeletal Muscle*. San Luis Obispo: California Polytechnic State University; 2012:80. Available at: <http://digitalcommons.calpoly.edu/theses/914/>. Accessed October 8, 2014.
- [23] Medzhitov, Ruslan. "Origin and Physiological Roles of Inflammation." *Nature* 454.7203 (2008): 428-35.

[24] “Autofluorescence: Causes and Cures.” *Wright Cell Imaging Facility*. University of Toronto, 04 April 2006.

[25] Carter, Perry. *The Cardiovascular System: Blood Vessels*. Midlands Technical College Science Department. Web. December 31, 2015.

APPENDIX A: Functional Vasodilation Protocol

Date _____ Functional Vasodilation with Trans-illumination Initials _____

Mouse Information

Age: _____
Sex: _____
Tag: _____
Genotype/strain: _____
Cage: _____

Purpose: _____

Materials

1. Standard pattern forceps (1)
2. Fine forceps- S&T (2)
3. Curved iris scissors (1)
4. Depilatory cream- Veet
5. Cotton swabs
6. Gauze sponges (2x2 and 4x4)
7. Chlorhexidine diacetate (Nolvasan)
8. Veterinary ointment
9. Surgical tape
10. FST heat pad w/ rectal probe
11. Petri dish w/ saline
12. Tungsten microelectrodes
13. Clay
14. Plastic wrap
15. Trans-illumination device
16. Data acquisition unit- PowerLab
17. Digital chart recording software- LabChart
18. Intravital microscope- Olympus BXFM
19. Digital imaging software- QCapturePro
20. Sodium nitroprusside (SNP)
21. 70% isopropyl alcohol (IPA)

Animal preparation

22. Place animal in induction chamber.
23. Open oxygen cylinder. Set flow high and isoflurane to 5%.
24. Once anesthetized, weigh animal and move to preparatory bench in a supine position.
25. Reduce isoflurane to 1-3% and flow to 0.5-1.5 l·min⁻¹.
26. Apply depilatory cream to hindlimb with a cotton swab and let sit for 1-3 minutes.
27. Spray a 2x2 gauze sponge with Nolvasan and wipe hindlimb clean of cream and hair.
28. Flip animal over and use clippers to shave the hair from the posterior sides of the hindlimbs.
29. Complete hair removal with depilatory cream.
30. Cover heat pad with a 4x4 gauze sponge and transfer animal to surgery stage.
31. Apply veterinary ointment to rectal probe and insert. Set thermo-controller to 35°C.

Surgical exposure

32. Make a small incision on the middle, medial aspect of the left hindlimb.
33. Insert the closed scissors underneath the skin and open them repeatedly to separate the skin from connective tissue.
34. Cut away the skin above the gracilis muscles and the collateral circuit.
35. Blunt dissect and remove the connective tissue overlying the gracilis muscle.
36. Position the trans-illumination LED probe underneath the limb, below the gracilis.
37. Turn on the PowerLab and open LabChart.
38. Open the Isolated Stimulator Panel and set the frequency to 1 Hz, the duration to 200 μ s, and the current to 1 mA.
39. Hook the microelectrodes up to the isolated stimulator attached to the PowerLab.
40. Use clay to hold the wires at the base of the electrodes in place.
41. Position the electrodes with the tips resting on the surface of the gracilis anterior (~1 cm apart, between the saphenous and profunda).
42. Turn on the stimulator and start stimulation.
43. Adjust electrode placement and current for a maximal localized contraction, and then stop stimulation.
44. Apply saline to tissue, cover preparation with plastic wrap, and equilibrate for 30 minutes.

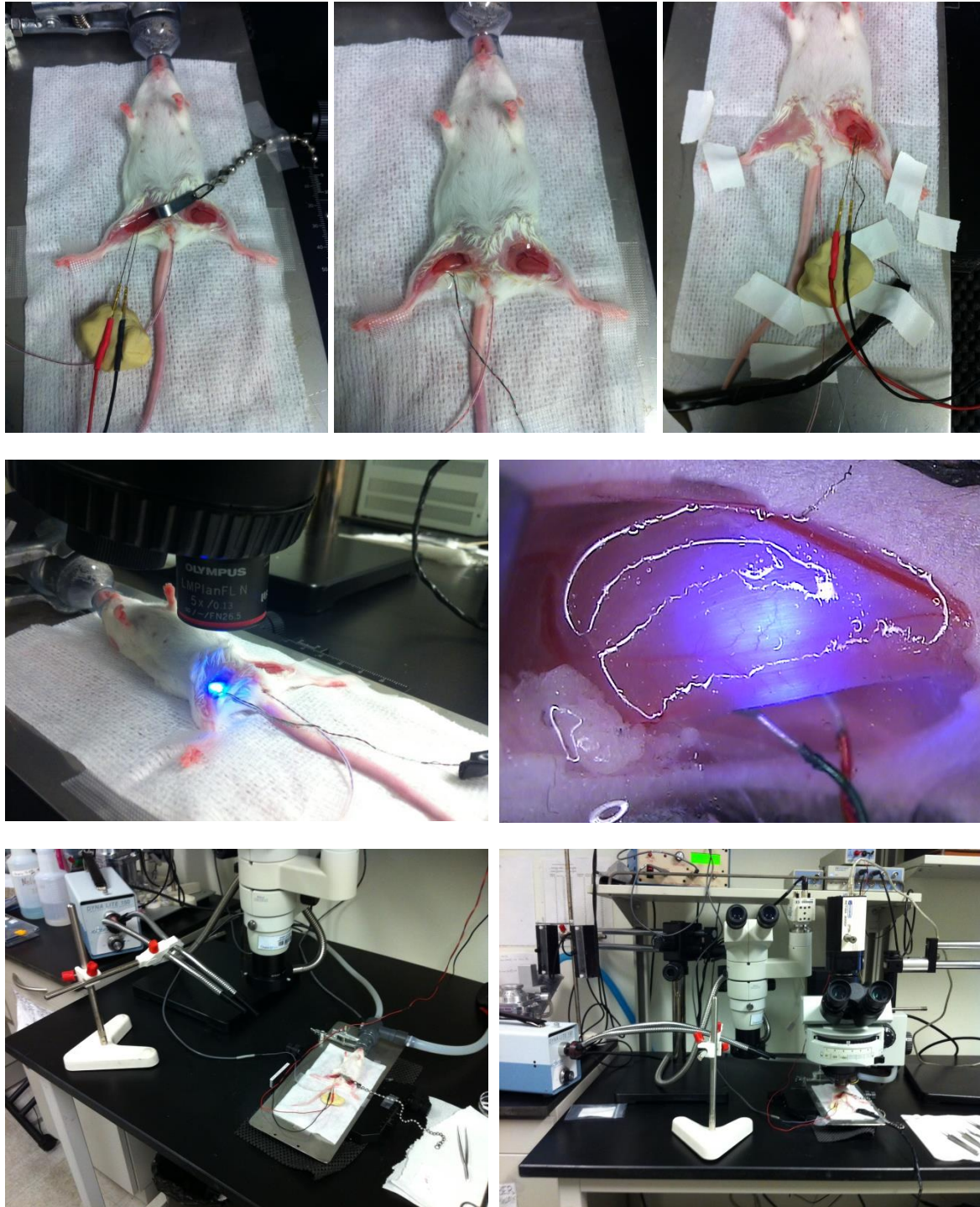
Functional Vasodilation

45. In LabChart, change the frequency to 8 Hz.
46. Switch on the trans-illumination and adjust the brightness using the dimmer switch.
47. Open QCapturePro and position the intravital microscope above the collateral arteriole.
48. Acquire resting images of both the arteriole and the profunda femoris artery.
49. Stimulate the muscle for 90 seconds.
50. Capture images of the collateral and the profunda immediately after stimulation (series of 10) and save all images acquired.
51. Maximally dilate with SNP and capture images of the collateral and the profunda.
52. Repeat the surgical exposure and functional vasodilation procedures on the control limb.

Post-Surgical

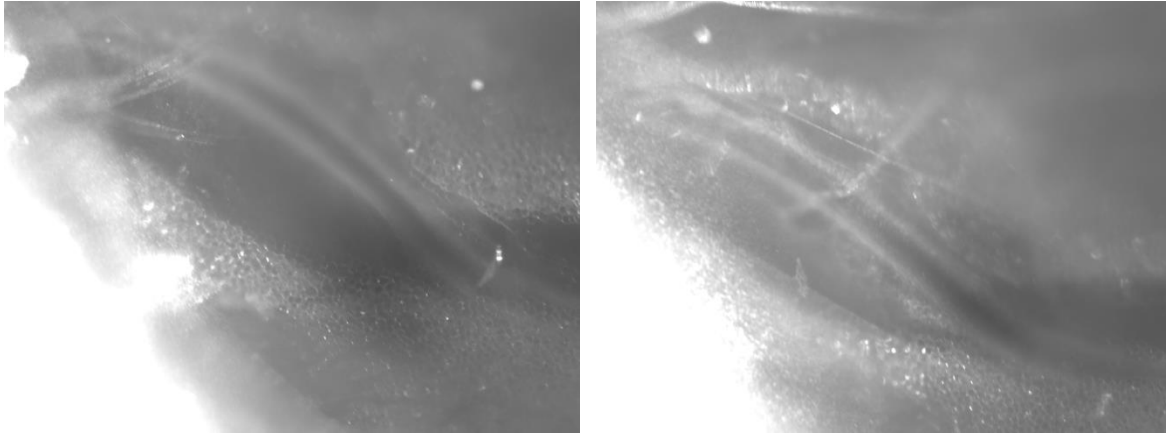
53. Perform cervical dislocation to euthanize the animal and dispose of in biohazard.
54. Turn off isoflurane, flow, and close oxygen.
55. Wash all instruments used during procedure.
56. Wipe down the surgical area with IPA.

APPENDIX B: Experimental Set-Up

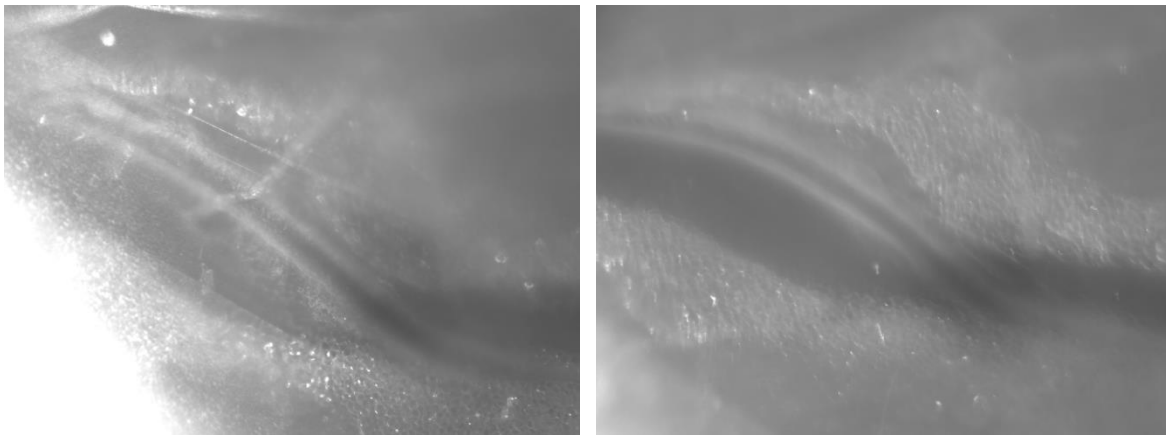


APPENDIX C: Sample Raw Images

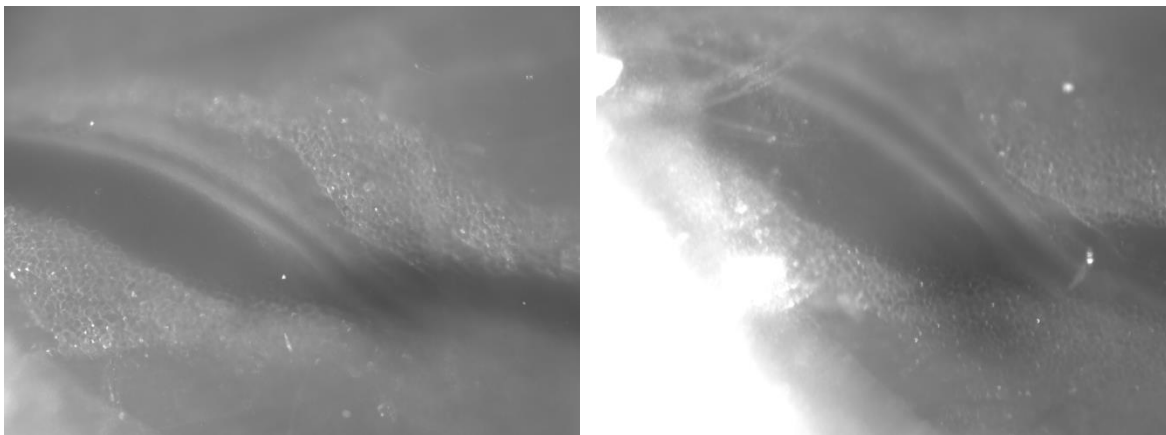
Profunda femoris artery, normal conditions – resting (left) and dilated (right)



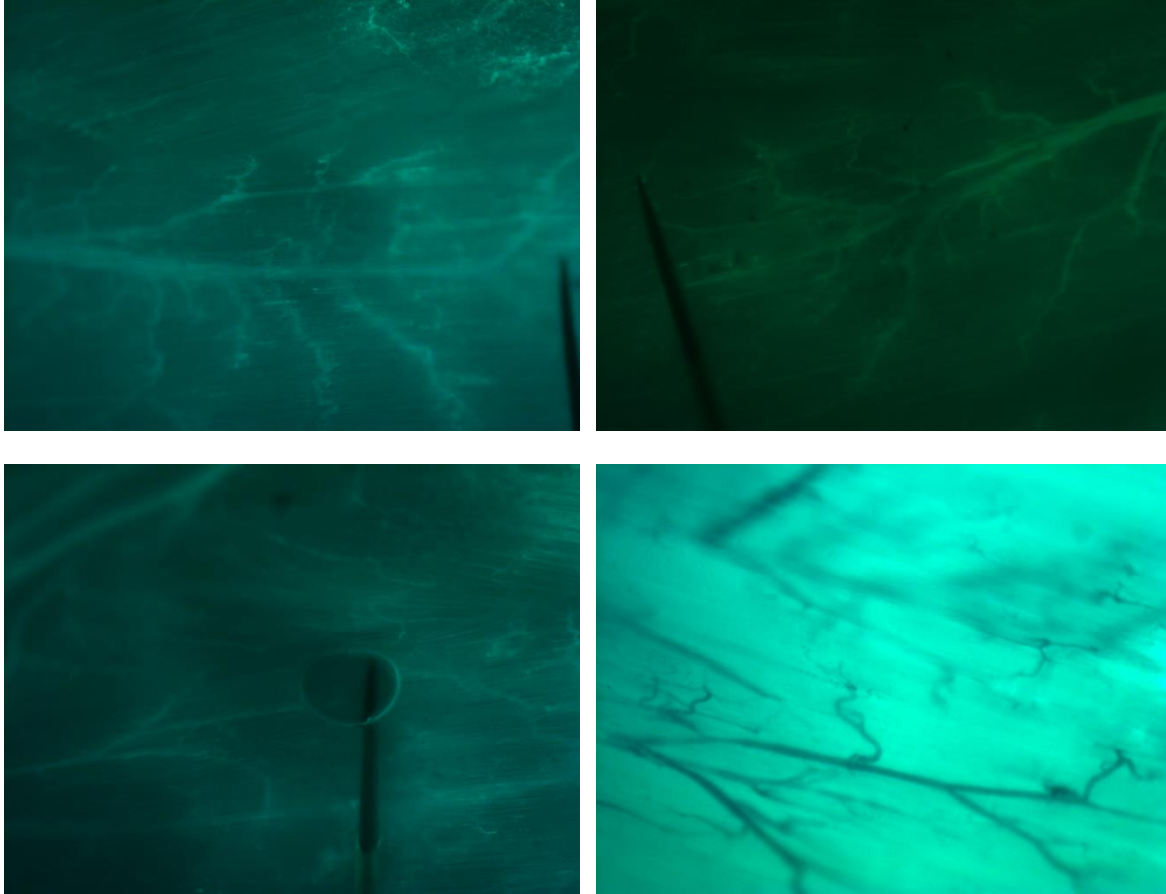
Profunda femoris artery, gracilis undermined – resting (left) and dilated (right)



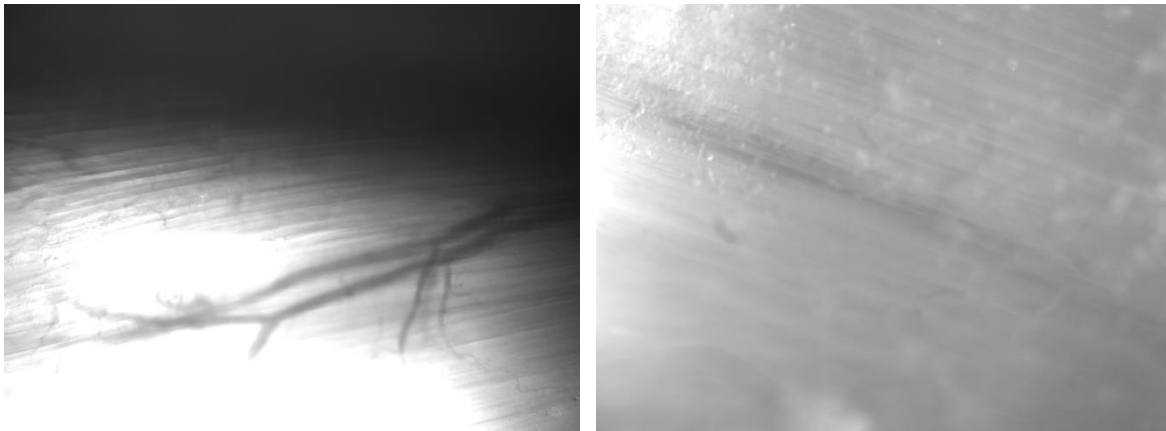
Profunda femoris artery, LED probe inserted – resting (left) and dilated (right)



Gracilis collateral midzone with FITC-dextran



Gracilis collateral midzone with trans-illumination device



APPENDIX D: Raw Data

	Normal			Gracilis undermined			LED probe		
Replicate	Resting (μm)	Dilated (μm)	% Change	Resting (μm)	Dilated (μm)	% Change	Resting (μm)	Dilated (μm)	% Change
1	58.23523468	111.1582473	90.87799	67.06680391	108.5021362	61.78218	60.89134572	102.326678	68.04798
2	72.34582461	102.326678	41.44103	78.52128279	97.94409481	24.73573	79.41772027	103.2231155	29.97492
3	70.58615104	77.62484531	9.971778	82.04062993	108.5021362	32.25415	86.45641454	106.7424627	23.4639
4	66.60198447	100.1353864	50.34895	75.00193565	109.8301917	46.43648	62.65101929	94.39154629	50.66243
5	74.10549818	109.3985737	47.62545	64.41069286	108.5021362	68.45361	71.44938713	101.4634419	42.00743
6	67.06680391	98.8073309	47.32673	69.68971356	97.94409481	40.54312	69.68971356	95.28798377	36.73178
7	67.49842195	103.2231155	52.92671	73.67388013	95.71960181	29.92339	74.10549818	107.2072821	44.66846
8	48.97204741	72.34582461	47.72881	57.80361663	81.60901188	41.18323	58.23523468	82.04062993	40.87799

APPENDIX E: Statistical Analysis

Paired T-Tests Comparing Resting and Dilated Diameters

Paired T-Test and CI: Rest (Normal), Dilated (Normal)

Paired T for Rest (Normal) - Dilated (Normal)

	N	Mean	StDev	SE Mean
Rest (Normal)	8	65.68	8.28	2.93
Dilated (Normal)	8	96.88	14.23	5.03
Difference	8	-31.20	12.88	4.55

95% CI for mean difference: (-41.97, -20.43)

T-Test of mean difference = 0 (vs ≠ 0): T-Value = -6.85 P-Value = 0.000

Paired T-Test and CI: Rest (Gracilis undermined), Dilated (Gracilis undermined)

Paired T for Rest (Gracilis undermined) - Dilated (Gracilis undermined)

	N	Mean	StDev	SE Mean
Rest (Gracilis undermine)	8	71.03	7.90	2.79
Dilated (Gracilis underm)	8	101.07	9.78	3.46
Difference	8	-30.04	9.12	3.22

95% CI for mean difference: (-37.66, -22.42)

T-Test of mean difference = 0 (vs ≠ 0): T-Value = -9.32 P-Value = 0.000

Paired T-Test and CI: Rest (LED probe), Dilated (LED probe)

Paired T for Rest (LED probe) - Dilated (LED probe)

	N	Mean	StDev	SE Mean
Rest (LED probe)	8	70.36	9.66	3.41
Dilated (LED probe)	8	99.09	8.32	2.94
Difference	8	-28.72	6.77	2.39

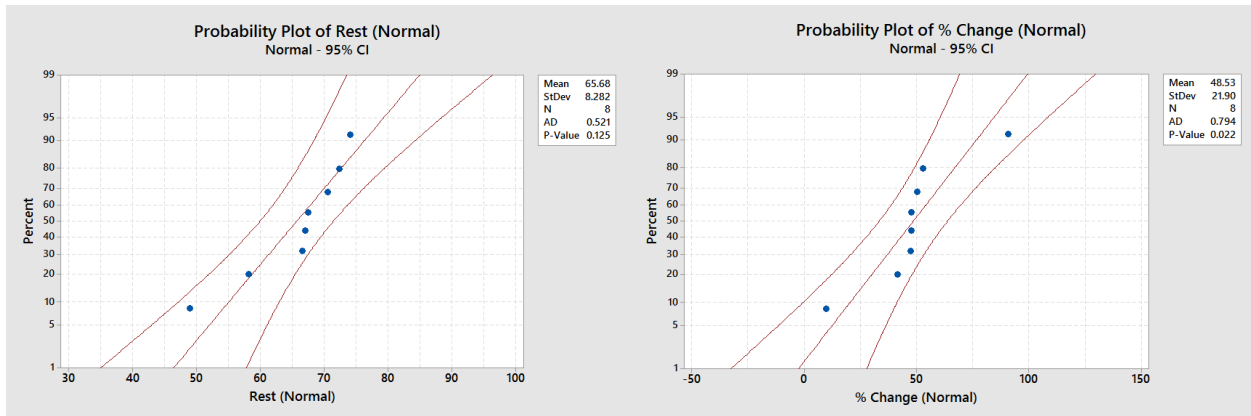
95% CI for mean difference: (-34.38, -23.06)

T-Test of mean difference = 0 (vs ≠ 0): T-Value = -12.00 P-Value = 0.000

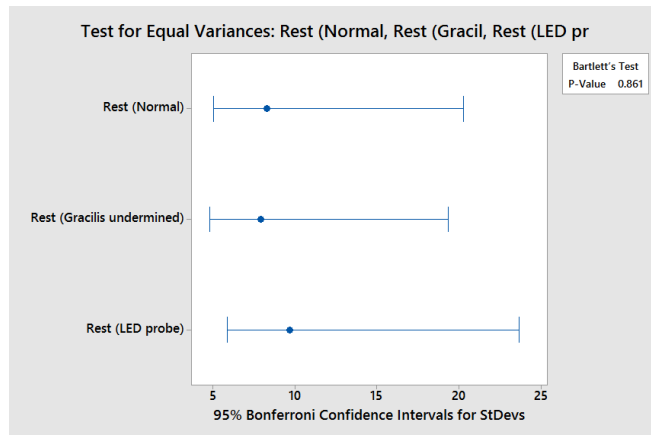
Anderson Darling Normality Test

	Normal			Gracilis undermined			LED probe		
	Resting (μm)	Dilated (μm)	% Change	Resting (μm)	Dilated (μm)	% Change	Resting (μm)	Dilated (μm)	% Change
Anderson-Darling p-value	0.125	0.057	0.022	0.974	0.063	0.502	0.852	0.192	0.674

Sample Normal Probability Plots



Bartlett's Test for Equal Variance and ANOVA [Resting Diameter]

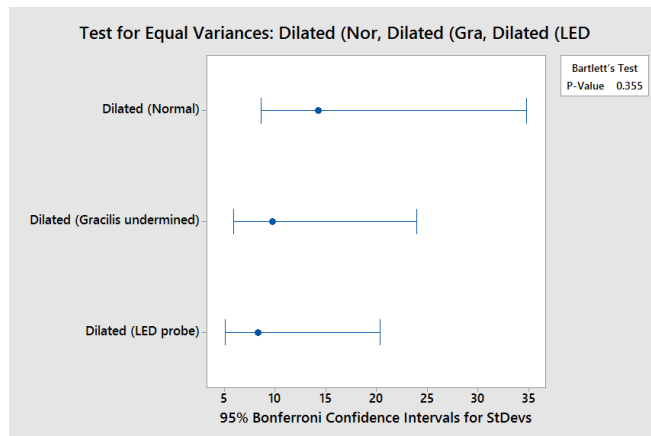


Nested ANOVA: Resting Diameter versus Group

Analysis of Variance for Resting Diameter

Source	DF	SS	MS	F	P
Group	2	136.0352	68.0176	0.910	0.418
Error	21	1569.4232	74.7344		
Total	23	1705.4585			

Bartlett's Test for Equal Variance and ANOVA [Dilated Diameter]

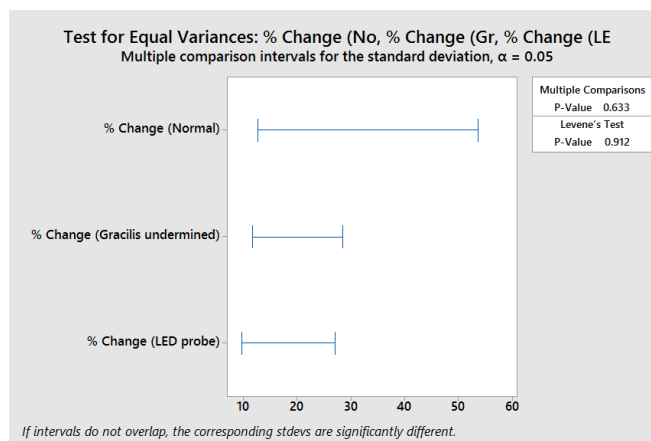


Nested ANOVA: Dilated Diameter versus Group

Analysis of Variance for Dilated Diameter

Source	DF	SS	MS	F	P
Group	2	70.3475	35.1738	0.287	0.753
Error	21	2571.6876	122.4613		
Total	23	2642.0352			

Levene's Test for Equal Variance and Kruskal-Wallis Test [Percent Change]*



Kruskal-Wallis Test: % Change versus Group

Kruskal-Wallis Test on % Change

Group	N	Median	Ave Rank	Z
Gracilis undermined	8	40.86	11.1	-0.67
LED probe	8	41.44	11.1	-0.67
Normal	8	47.68	15.3	1.35
Overall	24		12.5	

H = 1.81 DF = 2 P = 0.404

*When one or more data sets is not normal, Levene's Test can be used to determine equal variances and the Kruskal-Wallis Test can be used for comparison of medians.